



Human activities determine quantity and composition of dissolved organic matter in lakes along the Yangtze River



Dong Liu^a, Yingxun Du^a, Shujie Yu^b, Juhua Luo^a, Hongtao Duan^{a,*}

^a Key Laboratory of Watershed Geographic Sciences, Nanjing Institute of Geography and Limnology, Chinese Academy of Sciences, Nanjing, 210008, China

^b Ocean College, Zhejiang University, Zhoushan, 316021, China

ARTICLE INFO

Article history:

Received 10 May 2019

Received in revised form

29 August 2019

Accepted 24 September 2019

Available online 27 September 2019

Keywords:

Optical properties

Dissolved organic matter

Lake eutrophication

Yangtze river

Human activities

ABSTRACT

Dissolved organic matter (DOM) plays important roles in the aquatic biogeochemical cycle and the global carbon cycle. However, it is highly spatially and temporally varied due to complex sources from the catchment (allochthonous) and from within the system (autochthonous). Satellite remote sensing provides the ability to monitor DOM and identify the spatio-temporal variations in lakes on a global or regional scale. In this study, field work was conducted in 55 lakes in August 2012 along the middle and lower reaches of the Yangtze River (MLR-YR), where most lakes were characterized by eutrophication due to intense human activities. The results showed that both colored DOM (CDOM) and total DOM differed significantly by and were linearly related to the human-induced trophic state index (TSI), with $R^2 = 0.41$ and 0.61 , respectively. Autochthonous substances by phytoplankton contributed to 38.5% of CDOM and 35.2% of DOM, and allochthonous terrestrial substance indexed by land cover change and aquaculture contributed to almost half, with 49.7% of CDOM and 49.8% of DOM. In total, human activities explained as much as 81.7% and 87.5% of the variations in CDOM and DOM, respectively. Finally, a flowchart for estimating DOM from satellite-derived TSI was proposed. This study has great significance for synchronously monitoring and managing aquatic environment quality in regional eutrophic lakes around the world.

© 2019 Elsevier Ltd. All rights reserved.

1. Introduction

Dissolved organic matter (DOM), usually expressed by dissolved organic carbon (DOC, mg C/L), is a broad classification used to refer to organic molecules of various origin and composition, such as sugars, fatty acids and alkanes, and complex polymeric molecules within aquatic systems (Hirtle and Rencz, 2003; Manahan and Crisp, 1982); this material plays important roles in the aquatic biogeochemical cycle and the global carbon cycle. With an area that is only 0.7% that of oceans, global lakes bury nearly half of organic carbon as that of the world's oceans (Dean and Gorham, 1998). In fact, there are many published studies about DOM in lakes (Ackefors and Enell, 1994; Mendonca et al., 2017; Stedmon et al., 2006; Yao et al., 2016; Zhang et al., 2009, 2010). These studies reveal that DOM varies greatly in terms of the spatial and temporal scales of lakes, and this variation is impacted by human-induced eutrophication or external DOM from the drainage basin.

There are two DOM sources: autochthonous and allochthonous. Autochthonous DOM mainly comes from phytoplankton production. Aquatic phytoplankton can release extracellular DOM (Baines and Pace, 1991), and their degradation also produces DOM (Zhang et al., 2009). For global open oceans, DOM is greatly related to phytoplankton density (Morel and Gentili, 2009; Tiwari and Shanmugam, 2011). Allochthonous DOM from the drainage basin is also an important DOM source resulting from the decomposition processes of dead organisms such as plants. Allochthonous DOM is greatly impacted by external inputs because a considerable amount of DOM is transported into lakes from domestic and industrial sewage (Liu et al., 2015; Stedmon et al., 2006). In these cases, the DOM in lakes was often differed with tempo-spatially varied human activities (Jiang et al., 2013; Kutser, 2012; Sun et al., 2011).

Satellite remote sensing is an alternative choice for dynamically monitoring DOM in lakes. Generally, total DOM is divided into two parts: optically active and non-active components. The optically active DOM, namely the colored DOM (CDOM), has been widely studied using satellite data (Chen et al., 2017a; Fichot and Benner, 2011; Fichot et al., 2015; Morel and Gentili, 2009; Siegel et al.,

* Corresponding author.

E-mail address: htduan@niglas.ac.cn (H. Duan).

2002). Many empirical and semi-analytical remote sensing algorithms have been developed to estimate CDOM, not only for oceanic waters (Castillo and Miller, 2008; Morel and Gentili, 2009; Swan et al., 2013; Tiwari and Shanmugam, 2011) but also for inland waters (Chen et al., 2017b; Jiang et al., 2013; Kutser, 2012). In contrast, few algorithms have specifically focused on the optically non-active or total DOM that is usually quantified by DOC (Hirtle and Rencz, 2003; Liu et al., 2018). In fact, total DOM has been generally estimated from CDOM based on statistical correlation between both concentrations with average R^2 of ~0.84 (Castillo and Miller, 2008; Fichot and Benner, 2011; Fichot et al., 2015; Jiang et al., 2012; Liu et al., 2018), but most of these studies have been conducted for oceans, with little attention given to inland lakes. To remotely monitor CDOM and/or DOM in regional lakes, it is important to understand their optical properties. Moreover, knowledge of DOM variations with environmental factors is a prerequisite for the refinement of remote sensing algorithms (Oubelkheir et al., 2005).

Lake eutrophication is a global problem. Wang et al. (2018) reported that 63.1% of lakes with surface area >25 km² were in eutrophication globally. The middle and lower reaches of the Yangtze River (MLR-YR) is one representative region containing 696 lakes that are larger than 1 km² (Ma et al., 2010). Moreover, most lakes along the MLR-YR are significantly characterized by human-induced eutrophication (Duan et al., 2014; Ma et al., 2010; Zhang et al., 2007). To the best of our knowledge, no study has systematically analyzed the optical properties of DOM in these lakes, nor has remote sensing monitoring been used. In this study, we describe the optical properties of DOM, trophic state, and correlations between different variables in the lakes along the MLR-YR. The impact factors and composition of DOM are then discussed. Based on our findings, the implications for remote sensing monitoring DOM are also addressed.

2. Materials and methods

2.1. Study area

With a length of ~6300 km, the Yangtze River (locally called the "Changjiang River") is the longest river in China and the third longest river in the world (Wang et al., 2012). According to the geology, climate, and geomorphology, the Yangtze River is divided into the upper, middle and lower reaches (Chen et al., 2001). The MLR-YR starts from Yichang city, is ~1880 km in length, and has a low-gradient basin with a coverage area of ~785,000 km². With 696 lakes larger than 1 km² (Ma et al., 2010), the MLR-YR basin is a representative for the region with dense lakes. Lakes along the MLR-YR are shown in Fig. 1.

The MLR-YR basin is in the East Asian monsoon climate zone, with high temperature and heavy precipitation in summer but opposite conditions in winter (Guo et al., 2014). A large amount of terrestrial DOM is flushed into lakes in summer with high runoff, and lakes receive effluent discharges from agricultural activities as well as from small villages or mega-urban areas (Duan et al., 2014).

2.2. Field data collection

In August (summer), 2012, 55 lakes along the MLR-YR were investigated (Fig. 1). Table 1 shows the name, area, and water depth of each lake. In total, there were 161 sampled stations (Table 1). In each fieldwork episode, the Secchi disk depth (SDD) was measured at the ship's shaded side using a 25-cm diameter disk painted in black/white quarters; surface water within a 0–30-cm water depth was collected using a standard 2-liter polyethylene water sampler. All *in-situ* water samples were stored in brown bottles and on ice for approximately 4 h before filtration.

2.2.1. Constituent concentrations

The same *in-situ* raw water was used for the total nitrogen (TN), total phosphorus (TP), and chemical oxygen demand (COD) samples. *In-situ* water samples were also filtered through Satorius cellulose acetate filters (0.45- μ m pore size, Φ 47 mm) and the filter membrane with particle was used as the chlorophyll-a (Chl-a) sample. The TN and TP concentrations were determined by spectrophotometric analysis after persulfate digestion (APHA, 1995). The COD was determined using the potassium permanganate-boiling method (APHA, 1995). The Chl-a sample was first soaked in 90% ethanol in the dark for 24 h and heated to 80–90 °C for 3–5 min. The light absorbance of the extracting solution was then measured at 630 (A_{630}), 645 (A_{645}), 663 (A_{663}), and 750 nm (A_{750}) using a UV2401 Spectrophotometer. Finally, the Chl-a concentration was calculated using Eq. (1) (Knap et al., 1996).

$$\text{Chl} - a = (11.64(A_{663} - A_{750}) - 2.16(A_{645} - A_{750}) + 0.1(A_{630} - A_{750}))V_1/V_2 \times L \quad (1)$$

Where, V_1 is extracting solution volume (mL); V_2 is the filtration volume of *in-situ* raw water (L); and L denotes the optical path of a cuvette, $L = 1$ cm.

In-situ water samples were also filtered through pre-combusted (500 °C for 4 h) Whatman glass fiber filters (GF/F, 0.7- μ m pore size, Φ 47 mm) to collect DOM samples. Using HCl (2 mol/L), all samples were acidified to remove dissolved inorganic carbon (Knap et al., 1996). Then, DOM (or DOC) concentration was measured via the high temperature combustion method (680 °C) using a Shimadzu TOC-V total organic carbon analyzer (Knap et al., 1996).

2.2.2. CDOM absorption and fluorescence

The DOM sample was further filtered through a pre-rinsed Millipore polycarbonate filter (0.22- μ m pore size, Φ 47 mm) to collect the CDOM sample. In the lab, the CDOM absorption coefficient spectrum was measured from 250 nm to 800 nm with an interval of 1 nm using a Shimadzu UV2600 spectrophotometer (Mueller et al., 2003). The CDOM absorption coefficient exponentially decreases with increasing wavelength (Tiwari and Shanmugam, 2011; Zhang et al., 2010). With a known CDOM absorption coefficient at wavelength λ_0 ($a_{\text{CDOM}}(\lambda_0)$) and its spectral slope (S_{CDOM} , nm⁻¹), the absorption coefficient at any wavelength λ ($a_{\text{CDOM}}(\lambda)$) can be calculated using Eq. (2).

$$a_{\text{CDOM}}(\lambda) = a_{\text{CDOM}}(\lambda_0) \times \exp(-S_{\text{CDOM}}(\lambda - \lambda_0)) \quad (2)$$

For the CDOM samples from stations located at the lake centers, three-dimensional excitation-emission spectra (EEMs) were also measured by a Hitachi F-7000 fluorescence spectrometer with a 700-voltage xenon lamp (Hitachi High-Technologies, Japan). Ranges of 200–450 nm for excitation (5-nm intervals) and 250–600 nm for emission (1-nm intervals) were scanned. After Raman scattering elimination, excitation and emission calibration, inner-filter effect elimination, and fluorescence intensity normalization to quinine sulfate units (QSU), the EEMs were decomposed into individual fluorescent components by parallel factor analysis (PARAFAC) and the split-half validation procedure in MATLAB R2008a with DOM-Fluor toolbox (Zhang et al., 2010).

2.3. Lake watershed datasets

Similar to Mendonca et al. (2017), the watershed extent of each lake was identified through the WWF HydroBASINS tool provided by the USGS (www.hydrosheds.org). In the lake watershed extent definition, the HydroSheds dataset was processed with a user-

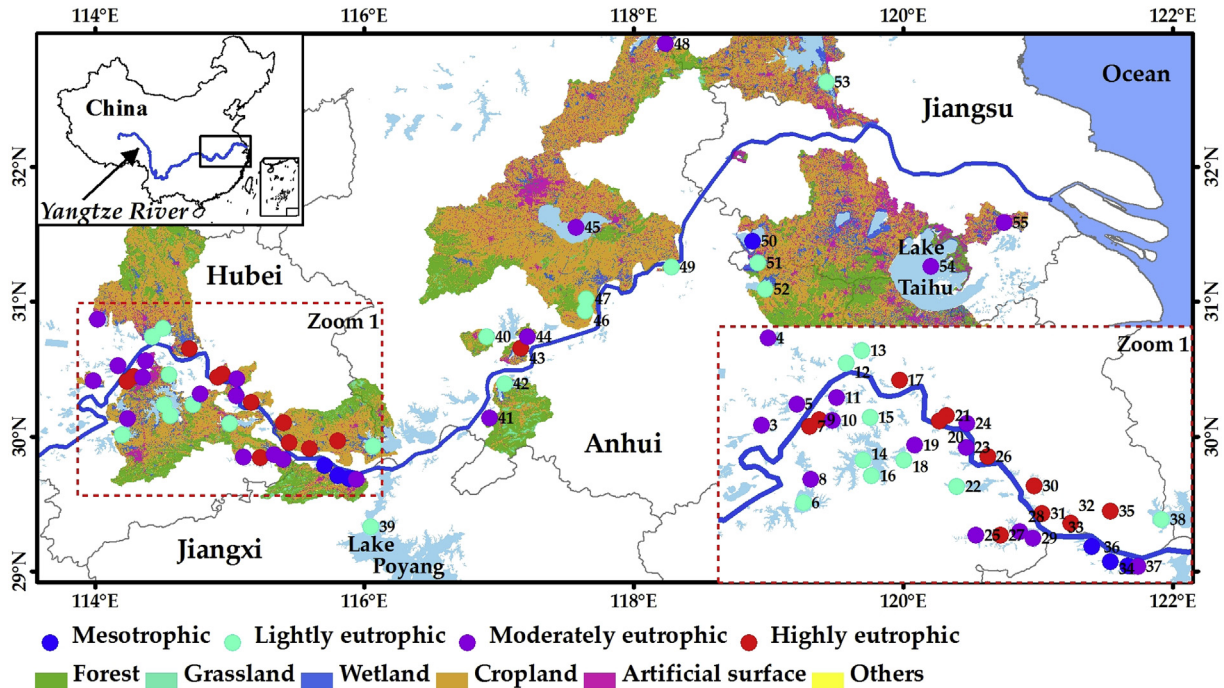


Fig. 1. Lakes along the MLR-YR. All lakes are located in the Hubei, Jiangxi, Anhui, and Jiangsu provinces, China. For different lake watersheds, areas of different land cover types are shown in [Supplementary Table S1](#). The administrative boundary data were sourced from the National Geomatic Center of China (www.ngcc.cn).

friendly graphical interface.

The lake watershed extent was used to extract the land cover in 2010 ([Table S1](#)). The land cover data were derived from the *Land Cover Atlas of the People's Republic of China* with 30-m resolution, which contained six land cover types (forest, grassland, wetland, cropland, artificial surface, and others) and were made available by the Institute of Remote Sensing Application, Chinese Academy of Sciences (CAS) (www.chinageoss.org).

The mean gross domestic product (GDP, 10^4 RMB/km²), population density (Pop, person/km²), and topsoil organic content (Soil-TOC, %weight) in each lake watershed were also calculated. Both the GDP and the population in 2010 were gridded reanalysis data and downloaded from the Global Change Research Data Publishing & Repository website (www.geodoi.ac.cn). The Soil-TOC data were extracted from the Harmonized World Soil Database based on the national soil survey of China in 1995 ([Shangguan et al., 2012](#)).

2.4. Trophic state index

There are many mathematical methods for assessing lake eutrophication. Among them, the simple and feasible trophic state index (TSI) is commonly used ([Aizaki et al., 1981](#); [Carlson, 1977](#); [Zhang et al., 2010](#)). The original TSI (TSI_O) was developed upon SDD, as relative indicator of algal biomass ([Carlson, 1977](#)). However, SDD is partially influenced by other factors like sediment resuspension, which is independent of algal biomass ([Aizaki et al., 1981](#); [Wang et al., 2002](#)). To make up for this deficiency, a modified TSI (TSI_M) was developed using Chl-a concentration as the indicator of algal biomass ([Aizaki et al., 1981](#)). Along the MLR-YR, most lakes are characterized by shallow waters and SDD is greatly impacted by sediment resuspension ([Duan et al., 2014](#); [Shi et al., 2015](#); [Xue et al., 2019](#)). Therefore, TSI_M was chosen in this study. Note that TSI_M may get different results with different inputs. In this case, the weighted arithmetic mean of TSI_M calculated from TN, TP, Chl-a, COD, and SDD was usually used to evaluate eutrophication of Chinese lakes

([Wang et al., 2002](#); [Zhang et al., 2006, 2010](#)). In this study, we also used the weighted arithmetic TSI_M (TSI for convenience), defined as Eq. (3) ([Zhang et al., 2006](#)):

$$TSI = \sum_{j=1}^m W_j \cdot TSI(j); \quad W_j = r_j^2 / \sum_{j=1}^m r_j^2$$

$$TSI(TN) = 10(5.453 + 1.694 \ln(TN))$$

$$TSI(TP) = 10(9.436 + 1.624 \ln(TP))$$

$$TSI(Chl - a) = 10(2.5 + 1.086 \ln(Chl - a))$$

$$TSI(COD) = 10(0.109 + 2.66 \ln(COD))$$

$$TSI(SDD) = 10(5.118 - 1.94 \ln(SD))$$
(3)

where TN, TP, Chl-a, COD, and SDD are used ($m = 5$). The weighted TSI also uses Chl-a as the basis; the Pearson's r_j of TN, TP, Chl-a, COD, and SDD to Chl-a are used to calculate the weight (W_j), respectively. The trophic levels are defined using TSI, with TSI <30 being oligotrophic, $30 \leq TSI < 50$ being mesotrophic, $50 \leq TSI < 60$ being lightly eutrophic, $60 \leq TSI < 70$ being moderately eutrophic, and $70 \leq TSI$ being highly eutrophic ([Wang et al., 2002](#); [Zhang et al., 2006](#)).

2.5. Multiple general linear model

To quantify the relative contribution of each explanatory variable to the spatial variations of the CDOM and DOM concentrations, correlation analyses and multiple general linear model (GLM) were used ([Tong et al., 2017](#)). DOM is affected not only by natural lake attributes but also by human activities in a lake's watershed ([Zhang et al., 2010](#)). Therefore, the explanatory variables included not only the area, water depth, and TSI in a lake but also the mean Soil-TOC, GDP, Pop, and percent area of artificial surface and cropland in the lake watershed (ACinLW). The lake area, water depth, and Soil-TOC represented natural variability, and the other variables represented human-induced disturbance intensity. Notably, p -value for each variable was also output, and $p < 0.05$ indicated a statistically

Table 1
Basic information for all surveyed lakes along the MLR-YR. For a specific lake, the symbol '/' denotes no available data. TL: trophic level; M: mesotrophic; IE: lightly eutrophic; mE: moderately eutrophic; hE: highly eutrophic. CDOM fluorescence was measured only for stations located at the lake center.

No.	Lake name	Longitude (°E)	Latitude (°N)	Area (km ²)	Depth (m)	Samples	TL	$a_{CDOM}(280)$ (m ⁻¹)	DOM (mg C/L)
1	Changhu	112.45	30.44	143.56	2.3	3	mE	/	5.43
2	Shangjin	112.51	29.64	13.86	3.6	3	hE	/	5.30
3	Xiaoshe	113.99	30.41	10.74	2.6	3	mE	14.51	4.69
4	Wangmu	114.02	30.86	7.93	2.2	3	mE	14.74	4.54
5	Sanjiao	114.17	30.52	2.22	2	3	mE	19.84	5.30
6	Futou	114.20	30.01	141.22	2.3	3	IE	/	3.67
7	Qingling	114.24	30.41	7.21	1.8	3	hE	23.33	8.42
8	Shangshe	114.24	30.13	10.24	1.8	3	mE	12.54	4.69
9	Huangjia	114.28	30.44	6.84	1.75	3	hE	19.22	5.25
10	Tangxun	114.35	30.44	44.83	2.3	3	mE	16.49	5.66
11	Wuhandong	114.38	30.56	34.22	4	3	mE	13.92	4.53
12	Baishui	114.43	30.74	15.39	5.6	3	IE	14.38	4.54
13	Wuhu	114.51	30.80	27.50	3.4	3	IE	15.44	5.01
14	Liangzi	114.51	30.23	349.76	3	3	IE	/	3.61
15	Baoxie	114.55	30.46	25.32	2	3	IE	10.69	4.61
16	Luhu	114.56	30.15	46.24	2.7	3	IE	11.56	4.23
17	Zhangdu	114.70	30.65	36.24	1.6	3	hE	15.26	6.20
18	Baoan	114.73	30.23	45.37	2.9	3	IE	10.24	3.66
19	Sanshan	114.78	30.31	23.90	2.6	3	mE	10.57	4.57
20	Huanggangdong	114.91	30.44	1.49	2.3	3	hE	18.67	5.93
21	Baitan	114.95	30.46	5.13	3	3	hE	16.74	6.52
22	Daye	115.00	30.10	73.60	4.1	3	IE	/	3.16
23	Huama	115.05	30.30	10.02	2.3	3	mE	/	5.07
24	Wangtian	115.05	30.42	5.88	3.1	3	mE	20.29	5.74
25	Nantan	115.10	29.84	8.60	3	3	mE	12.91	4.35
26	Cehu	115.16	30.25	9.06	2.3	3	hE	20.34	6.78
27	Zhulintang	115.23	29.84	3.30	2.7	3	hE	13.84	5.78
28	Wanghu	115.33	29.86	42.87	3.4	3	mE	12.30	4.43
29	Zhupo	115.40	29.83	17.40	6.4	3	mE	8.55	3.28
30	Chidong	115.40	30.10	40.49	4.3	3	hE	13.71	4.29
31	Makou	115.44	29.95	3.16	3.1	3	hE	13.28	6.48
32	Wushan	115.59	29.91	15.77	1.7	3	hE	24.72	7.22
33	Chihu	115.70	29.78	58.69	3.5	2	M	8.43	2.92
34	Changgang	115.80	29.71	56.09	1.6	3	M	9.51	1.94
35	Taibai	115.80	29.97	27.42	2.3	3	hE	22.28	6.56
36	Saicheng	115.89	29.68	56.09	5.6	3	M	7.07	2.21
37	Bali	115.94	29.68	17.29	4.7	3	mE	17.92	3.77
38	Longgan	116.06	29.92	295.54	3	3	IE	/	3.47
39	Poyang	116.16	29.36	3192.00	7.6	3	IE	11.11	1.91
40	Sanyashi	116.91	30.74	7.92	2.5	3	IE	17.43	4.73
41	Huangni	116.93	30.14	6.90	2.4	3	mE	16.26	3.77
42	Shengjin	117.04	30.39	95.89	5	3	IE	10.42	3.29
43	Pogang	117.16	30.65	52.08	2.5	2	hE	21.69	6.93
44	Liancheng	117.21	30.74	8.68	3.6	3	mE	16.03	3.74
45	Chaohu	117.57	31.55	787.97	2.5	2	mE	14.60	4.47
46	Fengsha	117.64	30.93	16.98	3.9	3	IE	14.65	3.65
47	Zhusi	117.65	31.02	11.36	2.7	3	IE	19.41	4.90
48	Qili	118.24	32.91	43.29	4.4	2	mE	18.80	2.60
49	Longwo	118.28	31.25	7.78	10	3	IE	12.72	3.55
50	Shijiu	118.88	31.45	214.31	5.3	3	M	7.71	3.27
51	Gucheng	118.92	31.28	31.22	4.3	3	IE	11.72	3.82
52	Nanyi	118.98	31.09	197.84	4.4	3	IE	12.12	2.57
53	Shaobo	119.43	32.63	103.47	1.8	3	IE	20.86	4.04
54	Taihu	120.21	31.26	2444.75	3.1	3	mE	15.87	3.94
55	Kuncheng	120.75	31.59	17.51	2.1	3	mE	19.66	3.78

significant contribution.

3. Results

3.1. General characteristics

All TN, TP, Chl-a, COD, and SDD spanned wide ranges in lakes along the MLR-YR (Table 2). The maximum values of these variables were 7.13, 37.5, 36.64, 4.57, and 15.4 times those of the minimum values, respectively (Table 2). Both TN and TP accelerated phytoplankton production and were significantly positively correlated with Chl-a, with Pearson's $r = 0.61$ and 0.6 , respectively (Fig. 2a).

The COD was also significantly positively related to Chl-a, with $r = 0.76$ and $p < 0.01$ (Fig. 2b). Note that the increased phytoplankton significantly decreased the SDD, with $r = -0.36$ and $p < 0.01$ (Fig. 2b). With significant relations to Chl-a, the TSI values at all stations were calculated by Eq. (3) and the arithmetic mean was further calculated for each lake (Table 1).

Lakes along the MLR-YR were characterized by serious eutrophication. For the 55 lakes investigated, none were oligotrophic, 4 were mesotrophic, 18 were lightly eutrophic, 20 were moderately eutrophic, and as many as 13 were highly eutrophic (Table 1). Lake eutrophication was spatially varied, and eutrophication in Hubei Province was generally more serious than that in the other

Table 2
Statistical values of different variables. 'std' denotes the standard deviation.

Variables	Minimum	Maximum	Mean \pm std
TN (mg/L)	0.45	3.21	1.52 \pm 0.63
TP (mg/L)	0.02	0.75	0.19 \pm 0.19
Chl-a (μ g/L)	7.06	258.71	77.15 \pm 56.24
COD (mg/L)	2.32	10.61	5.58 \pm 1.92
SDD (m)	0.10	1.54	0.55 \pm 0.28
$a_{\text{CDOM}}(280)$ (m^{-1})	5.97	27.73	15.37 \pm 4.77
DOM (mg C/L)	1.91	8.42	4.58 \pm 1.38
TSI	43.21	78.94	62.16 \pm 8.77
GDP (10^4 RMB/km 2)	166.73	9188.42	1149.58 \pm 1541.52
Population (person/km 2)	108.93	1536.9	523.28 \pm 267.56
Soil-TOC (%)	0.65	1.81	1.05 \pm 0.26
ACinLW (%)	19.14	93.33	66.67 \pm 17.72

provinces (Figs. 1 and S1a). The mean TSI values were 64.4 ± 9.14 , 52.23 ± 7.25 , 57.73 ± 6.01 , and 59.13 ± 5.98 in the Hubei, Jiangxi, Anhui, and Jiangsu provinces, respectively (Fig. S2 in the supplementary material file). It is also worth noting that 12 of the 13 highly eutrophic lakes were located in Hubei Province (Fig. 1).

3.2. Optical properties of DOM

The DOM concentrations in lakes along the MLR-YR were largely spatially varied. For different lakes, the DOM ranged from 1.91 to 8.42 mg C/L, with a mean \pm std of 4.58 ± 1.38 mg C/L (Table 2). The DOM was generally high in Hubei Province and decreased from upstream to downstream with increasing longitude (Figs. 3a and S1b). Similar to Zhang et al. (2010), we used the CDOM absorption coefficient at 280 nm ($a_{\text{CDOM}}(280)$) to denote the CDOM

concentration. The maximum $a_{\text{CDOM}}(280)$ was 4.64 times the minimum value, with a mean \pm std of $15.37 \pm 4.77 \text{ m}^{-1}$ (Table 2). However, the $a_{\text{CDOM}}(280)$ did not show significantly high values in lakes in Hubei Province like those found for the DOM (Figs. 3 and S1c). With $R^2 = 0.46$ for the linear relationship between $a_{\text{CDOM}}(280)$ and DOM, the $a_{\text{CDOM}}(280)$ only explained 46% of the variation in the DOM (Fig. 2d).

Four fluorescent components were identified by EEMs-PARAFAC analyses (Fig. 4). Component 1 (C1) had excitation (275 nm) and emission (308 nm) characteristics, which were similar to those of autochthonous tyrosine-like DOM (Coble, 1996). Component 2 (C2) displayed two excitation maxima (<250 and 310 nm) and a single emission maximum (392 nm), similar to autochthonous marine humic-like DOM caused by phytoplankton degradation (Coble, 1996). Component 3 (C3) had excitation (<250 nm and 285 nm) and emission (340 nm) features similar to autochthonous tryptophan-like DOM (Coble, 1996). Component 4 (C4) displayed excitation (245 and 355 nm) and emission (468 nm) characteristics similar to those of allochthonous terrestrial humic-like DOM (Coble, 1996).

All optical properties of DOM differed with TSI. Both $a_{\text{CDOM}}(280)$ and DOM were significantly linearly positively related to TSI, with $R^2 = 0.41$ and 0.61, respectively (Fig. 2c); for DOM, the mean \pm std was 2.59 ± 0.53 mg C/L, 3.8 ± 0.78 mg C/L, 4.42 ± 0.78 mg C/L, and 6.28 ± 0.99 mg C/L for the mesotrophic, lightly eutrophic, moderately eutrophic, and highly eutrophic lakes, respectively (Fig. 3c). For $a_{\text{CDOM}}(280)$, the mean \pm std was $8.18 \pm 0.91 \text{ m}^{-1}$, $13.77 \pm 3.3 \text{ m}^{-1}$, $15.32 \pm 3.17 \text{ m}^{-1}$, and $18.59 \pm 3.83 \text{ m}^{-1}$, respectively (Fig. 3c). All CDOM fluorescent components also increased with increasing trophic levels, especially for C2, C3, and C4 (Fig. 3d).

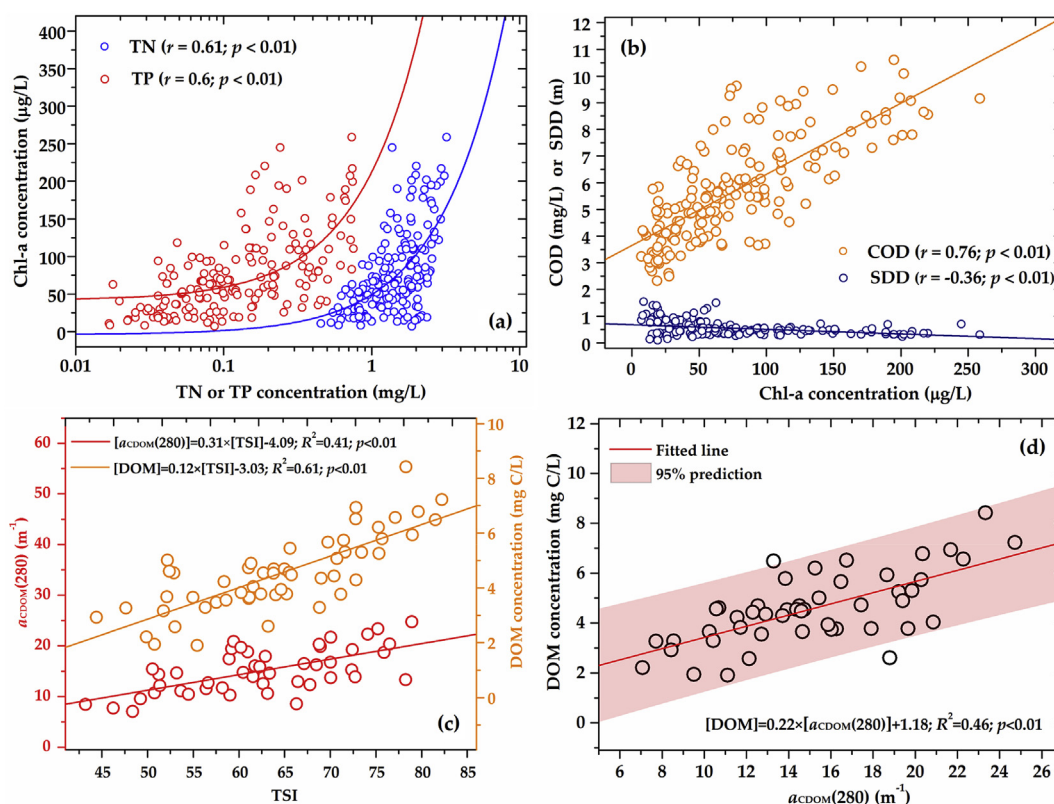


Fig. 2. The linear relationships between different *in-situ* variables: (a) between Chl-a and nutrients (TN and TP); (b) between COD, SDD and Chl-a; (c) between DOM composition ($a_{\text{CDOM}}(280)$ and DOM) and TSI; (d) between $a_{\text{CDOM}}(280)$ and DOM. In (a) and (b), all values at different stations were used. In (c) and (d), mean values of different lakes were used.

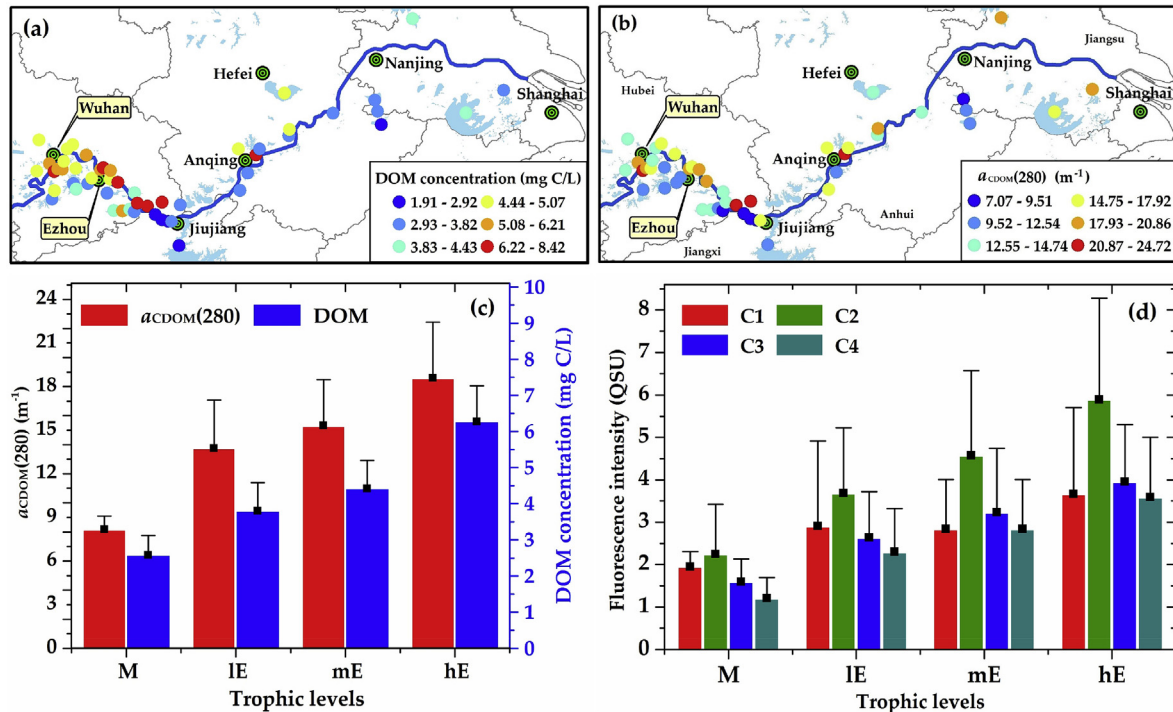


Fig. 3. Spatial distributions of DOM composition. (a) Mean DOM concentration; (b) Mean $a_{CDOM}(280)$; (c) Mean \pm std of $a_{CDOM}(280)$ and DOM for lakes with different trophic levels; (d) Mean \pm std of fluorescence intensity of lakes with different trophic levels. TL: trophic level; M: mesotrophic; IE: lightly eutrophic; mE: moderately eutrophic; hE: highly eutrophic.

3.3. Impact factors for DOM variations

The lake environment variables were greatly varied along the MLR-YR. For different lakes, mean \pm std of water depth, area, and TSI were 3.29 ± 1.56 m, 3.36 ± 1.58 km², and 62.16 ± 8.77 , respectively (Tables 1 and 2). For different lake watersheds, mean \pm std of GDP, population density, Soil-TOC, and ACinLW were $1149.58 \pm 1541.52 \times 10^4$ RMB/km², 523.28 ± 267.56 person/km², $1.05 \pm 0.26\%$, and $66.67 \pm 17.72\%$, respectively (Table 2). From upstream to downstream with increasing longitude, the mean GDP and Soil-TOC significantly increased ($p < 0.05$); however, the ACinLW in the lake watershed significantly decreased (Fig. S3 in the supplementary material file).

There were significant linear relationships between the lake environment variables and the optical properties of DOM. The lake area, water depth, and Soil-TOC were significantly negatively related to $a_{CDOM}(280)$, DOM, C2, C3, and C4 (Table 3). The ACinLW and TSI showed significant positive relationships with the $a_{CDOM}(280)$, DOM, C2, C3, and C4 (Table 3). However, the population density was only significantly positively correlated with C3, and GDP did not show a significant relation to any optical properties of DOM (Table 3). These relationships denoted the impacts of environmental variables on DOM composition.

4. Discussion

4.1. Human-induced DOM variations

For lakes distributed worldwide, Sobek et al. (2007) reported that the possible DOM range for a specific region was set by climatic and topographic features. For a specific lake, however, the lake watershed properties could also regulate the DOM (Sobek et al., 2007). All lakes along the MLR-YR were affected by the East Asian monsoon climate, with high precipitation in summer (Guo et al.,

2014). However, the MLR-YR region is one of the most developed regions in China, with a high population density (Yue et al., 2005). Being influenced by intense human activities (Bennett et al., 2001; Qin, 2002), the DOM in lakes along the MLR-YR was spatially varied with human-induced eutrophication (Fig. 3).

The lake area, water depth, and Soil-TOC in a lake watershed were used to describe the natural impacts on the spatial variations in DOM. The mean DOM in different lakes along the MLR-YR was 4.58 ± 1.38 mg C/L (Table 2), but the mean DOM in precipitation was only ~ 1.5 mg C/L in the MLR-YR region (Safieddine and Heald, 2017). Therefore, precipitation would dilute the DOM in lakes. For the Yangtze River, the DOM decreased with increasing water discharge, namely, precipitation (Liu et al., 2015). Negative relations between lake area, water depth and DOM composition also denoted the dilution impacts by precipitation (Table 3). For lake watersheds with high Soil-TOC, much of the terrestrial DOM could be flushed into rivers or lakes (Ludwig and Probst, 1996). If so, we supposed a positive relation between Soil-TOC and DOM composition, but the opposite occurred (Table 3). It might due to the negative relationship between Soil-TOC and ACinLW ($r = 0.48$; $p < 0.05$) and the positive relationship between ACinLW and DOM composition (Table 3). These indicated the insignificant impact of Soil-TOC on DOM.

The ACinLW, GDP, Pop, and TSI were used to describe the human impacts on spatial variations in DOM. Land cover had impacts on watershed DOM output, with a high value for cropland (Correll et al., 2001). For lakes along the MLR-YR, the cropland area percent in watershed also showed positive relations to DOM composition, with $r > 0$ (Fig. 5a). In addition, industrial and domestic sewage from human activities in a lake catchment would increase the riverine input of DOM (Stedmon et al., 2006; Xia and Zhang, 2011). All the artificial surface area percent, GDP, and Pop could indicate human activity intensity in lake watershed and showed increase effects on DOM composition (Fig. 5b, Table 3). For

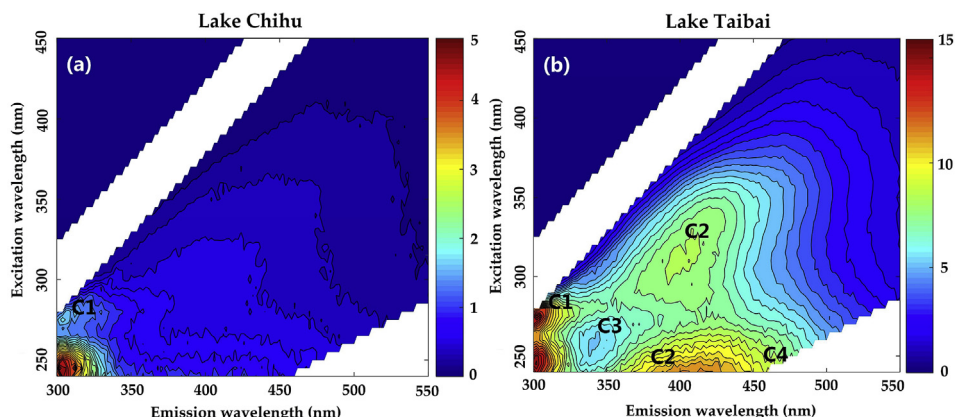


Fig. 4. EEMs-PARAFAC analysis results for water samples at (a) mesotrophic Lake Chihu and (b) highly eutrophic Lake Taibai. Fluorescence intensity is in QSU units. C1: autochthonous tyrosine-like DOM; C2: autochthonous marine humic-like DOM caused by phytoplankton degradation; C3: autochthonous tryptophan-like DOM; and C4: allochthonous terrestrial humic-like DOM.

Table 3

Pearson's r and significance levels of the linear relationships between DOM composition and environmental variables. Area: lake area; Depth: water depth; Soil-TOC: topsoil organic content (%weight); GDP: mean GDP in watershed (10^4 RMB/km²); Pop: mean population density in watershed (person/km²); ACinLW: area percent of artificial surface and cropland in lake watershed (%). Statistically significant contributions ($p < 0.05$) are annotated with a black filled square (■).

r	Ln(Area)	Depth	Soil-TOC	GDP	Pop	ACinLW	TSI
$a_{\text{CDOM}(280)}$	-0.33■	-0.46■	-0.30■	0.16	0.23	0.35■	0.64■
DOM	-0.50■	-0.50■	-0.61■	-0.03	0.20	0.49■	0.78■
C1	0.02	-0.13	-0.22	0.03	-0.01	0.21	0.21
C2	-0.32■	-0.31■	-0.42■	0.07	0.24	0.32■	0.46■
C3	-0.35■	-0.25	-0.52■	0.15	0.28■	0.40■	0.41■
C4	-0.33■	-0.31■	-0.37■	0.06	0.26	0.32■	0.51■

a specific lake watershed, because cropland area percent and artificial surface area percent were like a seesaw ($r = -0.5$; $p < 0.01$), so we combined them into ACinLW. The results showed that ACinLW was significantly positively related to DOM composition (Section 3.3). With increasing TSI, increased nitrogen and phosphorus from the basin elevated the nutrition available for potential phytoplankton growth (Bennett et al., 2001; Seitzinger et al., 2005; Xia and Zhang, 2011), and much DOM would be produced during phytoplankton degradation (Zhang et al., 2009, 2010). The CDOM in lakes of the Yungui Plateau, China, also differed with TSI (Zhang et al., 2010).

Contributions of different impact factors on DOM variations were quantitatively estimated by multiple GLM. Due to the unexpected relationship between Soil-TOC and DOM composition (Table 3), Soil-TOC was excluded in the multiple GLM analysis. The TSI significantly explained 65.7%, 74.3%, 33.3%, 51.4%, 26.2%, and 61.9% of the variations in the $a_{\text{CDOM}(280)}$, DOM, C1, C2, C3, and C4, respectively (Fig. 5c). In total, human activities explained as much as 81.7%, 87.5%, 64.4%, 70.5%, 71.2%, and 78.7% of variations in the $a_{\text{CDOM}(280)}$, DOM, C1, C2, C3, and C4, respectively (Fig. 5c). Overall, human activities dominated the spatial variations of DOM components in lakes along the MLR-YR.

4.2. DOM composition

Multiple GLM was also used to quantify the relative contributions of different components on DOM composition variations. Allochthonous terrestrial humic-like substance (C4) contributed almost half, with 49.7% of CDOM and 49.8% of DOM (Fig. 5d). Autochthonous marine humic-like substance (C2) contributed 20%

of CDOM and 15.7% of DOM; autochthonous tyrosine-like (C1) and tryptophan-like (C3) substances contributed 18.5% of CDOM and 19.5% of DOM, respectively (Fig. 5d). Overall, autochthonous substances contributed to 38.5% of CDOM and 35.2% of DOM in lakes along the MLR-YR.

Intense human activities increased the allochthonous terrestrial DOM input. On the one hand, human activities increased terrigenous DOM inputs to lakes by rivers. With a DOM stock of only 0.13 Tg C, Lake Taihu received as much as 0.24 Tg C/yr of terrestrial DOM from the input rivers (Hu et al., 2015). Compared with humic-like DOM, protein-like DOM from human activities was characterized by lower percent aromaticity (Weishaar et al., 2003; Zhang et al., 2010). $SUVA_{254}$, defined as the ratio of the CDOM absorption coefficient at 254 nm ($a_{\text{CDOM}(254)}$) to the DOM, denotes the DOM percent aromaticity (Weishaar et al., 2003). The increased $SUVA_{254}$ and percent aromaticity with increasing TSI indicated DOM contributions from human activities (Fig. S4). On the other hand, lake aquaculture also increased allochthonous DOM. For Nordic countries, Ackefors and Enell (1994) reported that approximately 80% of the organic matter in fish feed accumulated in waters. Along the MLR-YR, human activity intensity denoted by ACinLW was most strong in the Hubei Province and decreased from upstream to downstream (Fig. S3c); moreover, aquaculture yield was equivalent to 5.41, 4.87, 3.15, and 5.45 tons per hectare in the Hubei, Jiangxi, Anhui, and Jiangsu provinces in 2012, respectively (www.stats.gov.cn). These together resulted in the high values of eutrophication levels and DOM composition in the Hubei Province (Figs. 3 and S1).

Phytoplankton production was an important autochthonous source of DOM. Phytoplankton can release extracellular DOM (Baines and Pace, 1991), and their degradation can also produce DOM (Zhang et al., 2009). For eutrophic Lake Taihu (Fig. 1), phytoplankton production and decomposition are important contributors to CDOM (Yao et al., 2016; Zhang et al., 2009). The ratio of the CDOM absorption coefficient at 254 nm to that at 436 nm ($a_{\text{CDOM}(254)}/a_{\text{CDOM}(436)}$) indicates the CDOM source, with low values of 4.37–11.34 for allochthonous CDOM and higher values for autochthonous CDOM (Battin, 1998). A mean $a_{\text{CDOM}(254)}/a_{\text{CDOM}(436)}$ of 25.94 ± 7.58 indicated phytoplankton's important contribution to CDOM. With $R^2 = 0.31$ and $p < 0.01$, the significant positive relationship between $a_{\text{CDOM}(280)}$ and Chl-a also verified phytoplankton's contribution to CDOM (Fig. S5). Not only for CDOM, was phytoplankton production also an important source of total DOM. With $R^2 = 0.42$ and $p < 0.01$, the significant positive

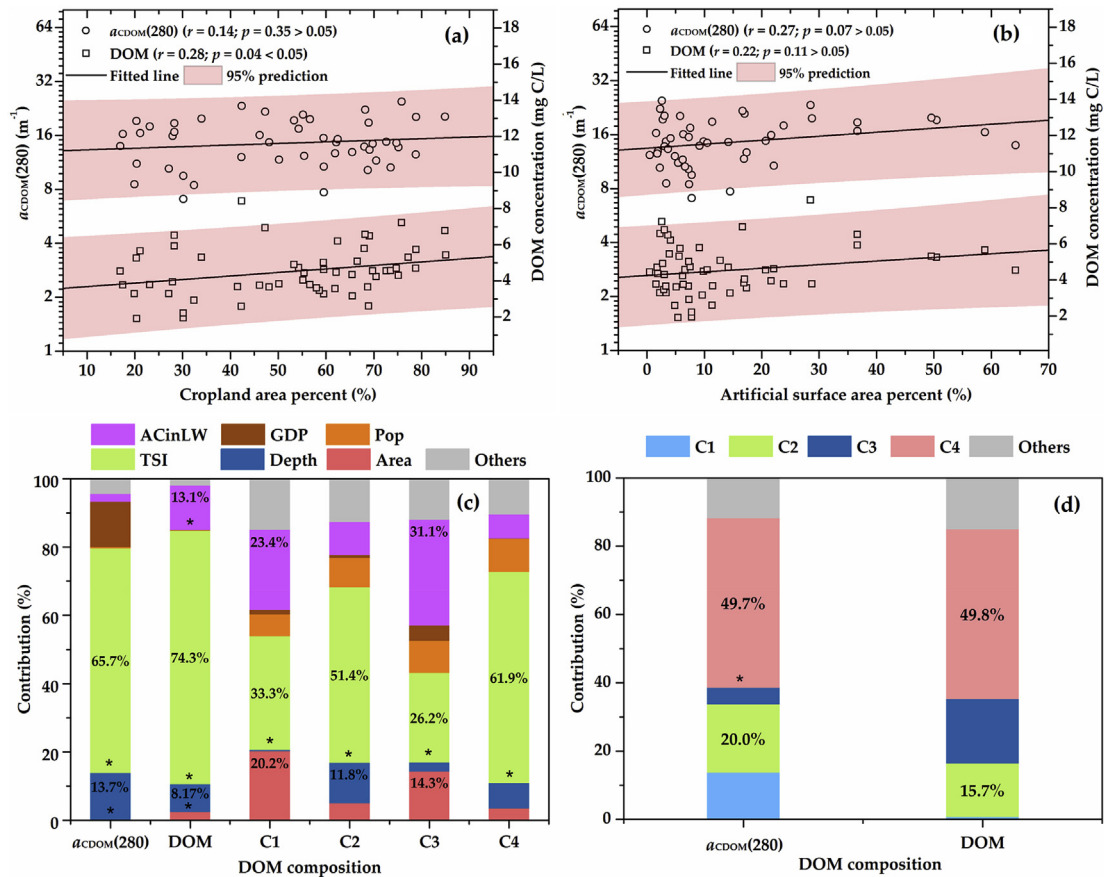


Fig. 5. Impacts on DOM composition variations. The linear relationships (a) between DOM composition and cropland area percent and (b) between DOM composition and artificial surface area percent. (c) Contributions of different impact factors. (d) DOM composition. Area: lake area; Depth: water depth; Pop: mean population density in watershed (person/km²); GDP: mean GDP in watershed (10⁴ RMB/km²); ACinLW: area percent of artificial surface and cropland in lake watershed (%). Statistically significant contributions ($p < 0.05$) are annotated with asterisks (*).

relationship between DOM and Chl-a verified phytoplankton's contribution to DOM (Fig. S5). For lakes located in the Sierra Nevada mountains, Spain, phytoplankton intensity was also reported as one driver of the DOM pattern (Mladenov et al., 2008).

4.3. Implications for remotely monitoring DOM

For lakes along the MLR-YR, it is unfeasible to calculate DOM from satellite-derived CDOM. First, it is difficult to derive CDOM from space. Due to eutrophication, sediment resuspension, and terrestrial material input, CDOM absorption often accounts for a small proportion of total light absorption in inland waters. For lakes along the MLR-YR (Fig. 1), CDOM absorption contributed around 20% (Xue et al., 2019); moreover, light absorption was dominated by non-algal particles, which had similar light absorption features as those of CDOM (Xue et al., 2019). Second, there was a strong correlation between CDOM and DOM at the ultraviolet band (Fig. 6a), but the atmospheric absorption at the ultraviolet band was strong and resulted in a weak signal to the satellite (Deluise, 1997). Moreover, because of no available ultraviolet satellite data, previous studies on CDOM retrieval usually used visible bands (Chen et al., 2017a; Siegel et al., 2002; Sun et al., 2011). At visible wavelengths with wavelength larger than 400 nm, however, the DOM was weakly related to the CDOM in lakes along the MLR-YR (Fig. 6a).

Alternatively, we could calculate the CDOM and DOM from the satellite-derived TSI. Human activities dominated DOM variations

in lakes along the MLR-YR (Section 4.1), and the TSI was significantly linearly related to both CDOM and DOM (Fig. 2c). Moreover, the TSI was significantly linearly related to the TSI(Chl-a), with $R^2 = 0.86$ and $p < 0.01$. For Chl-a in complex inland waters, many remote sensing algorithms have been proposed (Feng et al., 2014; Shi et al., 2015). For the largest freshwater Lake Poyang in the MLR-YR (Fig. 1), Feng et al. (2014) proposed the normalized green-red difference index using 560 nm and 681 nm. Therefore, CDOM and DOM could be estimated using satellite data by following the flowchart in Fig. 6b. Using the *in-situ* Chl-a, the uncertainty analyses of CDOM and DOM estimation are shown as Fig. 6c and d, respectively. With Chl-a estimation error of -50%–50%, mean absolute error (MAE) and mean relative error (MRE) of CDOM estimation were 21.6%–23.2% and -12.8%–9.4%, respectively (Fig. 6c); MAE and MRE of DOM estimation were 17.9%–23.1% and -19.1%–10.2%, respectively (Fig. 6d).

It is noteworthy that a high spatial resolution of satellite data is needed. On the one hand, high spatial variability often occurs in lake water environments (Duan et al., 2015; Jiang et al., 2013; Li et al., 2017). On the other hand, as shown in Table 1, many lakes along the MLR-YR are small (Ma et al., 2010). We recommend OLCI/Sentinel-3 satellite data with a full spatial resolution of 300 m × 300 m (<https://earth.esa.int>). Moreover, Sentinel-3A and Sentinel-3B form a two-satellite monitoring network that performs observations of the earth's surface once every 1.5 days. Therefore, the high temporal-spatial resolution of the OLCI/Sentinel-3 data

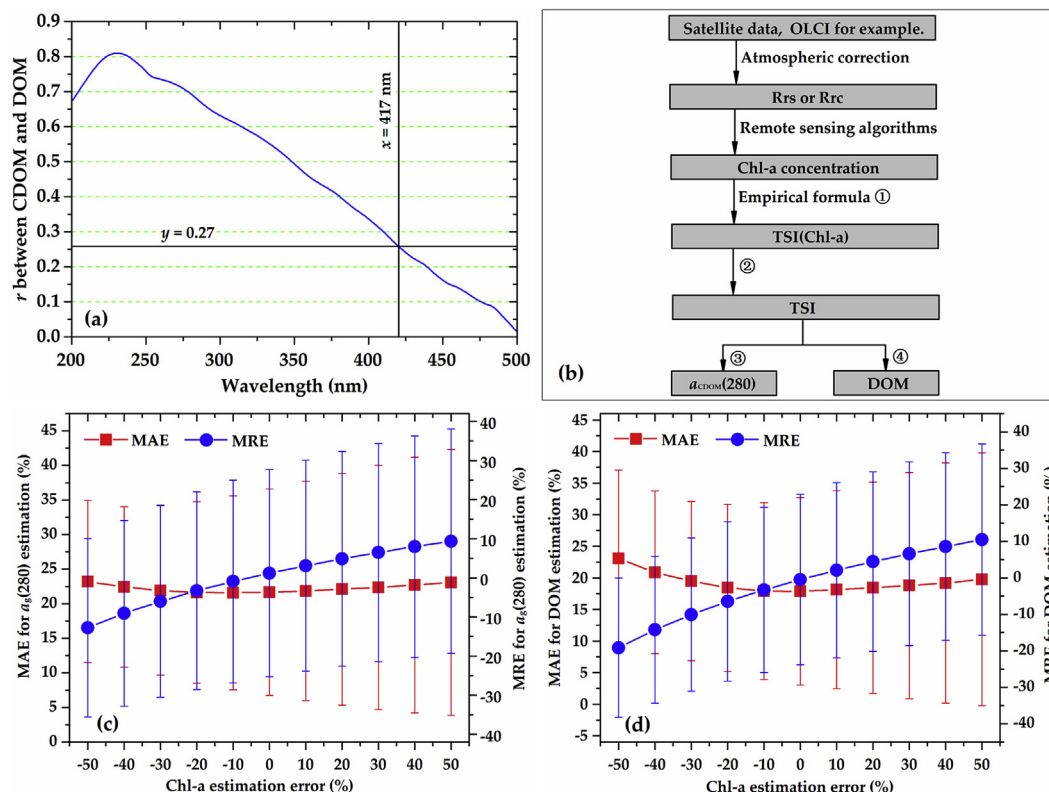


Fig. 6. Remote sensing estimation of DOM composition. (a) The Pearson's r between $a_{\text{CDOM}}(280)$ and DOM at different wavelengths. (b) One recommended flowchart for remotely monitoring DOM. ① is shown in Eq. (2); ② was $[\text{TSI}] = 0.85 \times [\text{TSI}(\text{Chl-a})] + 1.98$ ($N = 161$, $R^2 = 0.86$, $p < 0.01$), obtained from *in-situ* data of lakes along the MLR-YR; ③ and ④ are shown in Fig. 2c. (c) and (d) are uncertainty analyses for CDOM and DOM estimation with different Chl-a estimation errors.

have unique strengths in monitoring highly temporal-spatially varied lakes along the MLR-YR or other eutrophic lakes globally. Using the semi-analytical algorithms proposed by Xue et al. (2019), we estimated Chl-a from OLCI/Sentinel-3A in summer 2018 and further calculated $a_{\text{CDOM}}(280)$ and DOM using the recommended flowchart (Fig. 6b). The spatial distributions were consistent with the *in-situ* values in 2012, with high values for lakes in the Hubei Province (Figs. 3 and S6). In sum, we believed that the recommended flowchart was feasible for estimating $a_{\text{CDOM}}(280)$ and DOM in lakes along the MLR-YR.

5. Conclusions

Lakes along the MLR-YR were characterized by seriously eutrophic conditions. For all 55 lakes surveyed, no lake was characterized as oligotrophic, and lake eutrophication was correlated with local economic development. Under these conditions, the optical properties of DOM differed by TSI, and a significantly linear relationship was found between them. Human activities, such as domestic and industrial sewage discharge, land cover change, and aquaculture, also had significant effects on increasing allochthonous DOM. Allochthonous terrestrial humic-like substance (C4) contributed almost half, with 49.7% of CDOM and 49.8% of DOM. Phytoplankton production was also an important DOM source. Overall, autochthonous substances produced by phytoplankton contributed to 38.5% of CDOM and 35.2% of DOM. In total, human activities explained as much as 81.7% and 87.5% of the variations in $a_{\text{CDOM}}(280)$ and DOM, respectively. Based on the above findings, we recommended a flowchart to calculate the DOM in lakes along the MLR-YR from satellite-derived TSI using OLCI/Sentinel-3 satellite data.

Declaration of competing interest

The authors declare that they have no known competing financial interests or personal relationships that could have appeared to influence the work reported in this paper.

Acknowledgement

This study was supported by the Strategic Priority Research Program of the Chinese Academy of Sciences (Grant #XDA19040500), the National Natural Science Foundation of China (Grants #41901299, #41971309, #41671099, #41971314, #41671358 and #41431176), the Research Startup Project of Nanjing Institute of Geography and Limnology, Chinese Academy of Sciences (Grant #Y7SL051001), and the Natural Science Foundation of Jiangsu Province (Grants #BK20181102 and #BK20160049).

Appendix A. Supplementary data

Supplementary data to this article can be found online at <https://doi.org/10.1016/j.watres.2019.115132>.

References

- Ackefors, H., Enell, M., 1994. The release of nutrients and organic matter from aquaculture systems in Nordic countries. *J. Appl. Ichthyol.* 10, 225–241.
- Aizaki, M., Otsuki, A., Fukushima, T., Hosomi, M., Muraoka, K., 1981. Application of Carlson's trophic state index to Japanese lakes and relationships between the index and other parameters. *Int. Ver. Theor. Angew. Limnol.: Verh. Proc. Trav. SIL* 21, 675–681.
- APHA, 1995. In: *Standard Methods for the Examination of Water and Wastewater*, nineteenth ed. American Public Health Association, Washington, D. C.
- Baines, S.B., Pace, M.L., 1991. The production of dissolved organic matter by

- phytoplankton and its importance to bacteria: patterns across marine and freshwater systems. *Limnol. Oceanogr.* 36, 1078–1090.
- Battin, T.J., 1998. Dissolved organic materials and its optical properties in a black-water tributary of the upper Orinoco River, Venezuela. *Org. Geochem.* 28, 561–569.
- Bennett, E.M., Carpenter, S.R., Caraco, N.F., 2001. Human impact on erodable phosphorus and eutrophication: a global perspective. *Bioscience* 51, 227–234.
- Carlson, R.E., 1977. A trophic state index for lakes. *Limnol. Oceanogr.* 22, 361–369.
- Castillo, C.E.D., Miller, R.L., 2008. On the use of ocean color remote sensing to measure the transport of dissolved organic carbon by the Mississippi River Plume. *Remote Sens. Environ.* 112, 836–844.
- Chen, J., He, X., Zhou, B., Pan, D., 2017a. Deriving colored dissolved organic matter absorption coefficient from ocean color with a neural quasi-analytical algorithm. *J. Geophys. Res.: Oceans* 122 (11), 8543–8556.
- Chen, J., Zhu, W.-N., Tian, Y.Q., Yu, Q., 2017b. Estimation of colored dissolved organic matter from Landsat-8 imagery for complex inland water: case study of Lake Huron. *IEEE Trans. Geosci. Remote Sens.* 55, 2201–2212.
- Chen, Z., Li, J., Shen, H., Wang, Z., 2001. Yangtze River of China: historical analysis of discharge variability and sediment flux. *Geomorphology* 41, 77–91.
- Coble, P.G., 1996. Characterization of marine and terrestrial DOM in seawater using excitation-emission matrix spectroscopy. *Mar. Chem.* 51, 325–346.
- Correll, D.L., Jordan, T.E., Weller, D.E., 2001. Effects of precipitation, air temperature, and land use on organic carbon discharges from Rhode River watersheds. *Water Air Soil Pollut.* 128, 139–159.
- Dean, W.E., Gorham, E., 1998. Magnitude and significance of carbon burial in lakes, reservoirs, and peatlands. *Geology* 26, 535.
- Deluisi, J., 1997. *Atmospheric Ultraviolet Radiation Scattering and Absorption*. Springer Berlin Heidelberg.
- Duan, H., Feng, L., Ma, R., Zhang, Y., Arthur Loisselle, S., 2014. Variability of particulate organic carbon in inland waters observed from MODIS Aqua imagery. *Environ. Res. Lett.* 9, 084011.
- Duan, H., Loisselle, S., Zhu, L., Feng, L., Zhang, Y., Ma, R., 2015. Distribution and incidence of algal blooms in Lake Taihu. *Aquat. Sci.* 77, 9–16.
- Feng, L., Hu, C., Han, X., Chen, X., Qi, L., 2014. Long-term distribution patterns of chlorophyll-a concentration in China's largest freshwater lake: MERIS full-resolution observations with a practical approach. *Remote Sens.* 7, 275–299.
- Fichot, C.G., Benner, R., 2011. A novel method to estimate DOC concentrations from CDOM absorption coefficients in coastal waters. *Geophys. Res. Lett.* 38 (3).
- Fichot, C.G., Downing, B.D., Bergamaschi, B.A., Windham-Myers, L., Marvin-DiPasquale, M., Thompson, D.R., Gierach, M.M., 2015. High-resolution remote sensing of water quality in the San Francisco Bay-Delta estuary. *Environ. Sci. Technol.* 50, 573–583.
- Guo, W., Yang, L., Zhai, W., Chen, W., Osburn, C.L., Huang, X., Li, Y., 2014. Runoff-mediated seasonal oscillation in the dynamics of dissolved organic matter in different branches of a large bifurcated estuary-The Changjiang Estuary. *J. Geophys. Res.: Biogeosciences* 119, 776–793.
- Hirtle, H., Rencz, A., 2003. The relation between spectral reflectance and dissolved organic carbon in lake water: Kejimikujik National Park, Nova Scotia, Canada. *Int. J. Remote Sens.* 24, 953–967.
- Hu, Q., Wang, H., Li, J., Hu, C., Zhang, Y., Yu, T., Zhang, Y., 2015. Various inflows to Taihu lake in autumn: spectroscopy characteristics and DOM flux. *Environ. Sci. Technol.* 38, 152–158.
- Jiang, G., Ma, R., Duan, H., Loisselle, S.A., Xu, J., Liu, D., 2013. Remote determination of chromophoric dissolved organic matter in lakes, China. *Int. J. Digit. Earth* 7, 897–915.
- Jiang, G., Ma, R., Loisselle, S.A., Duan, H., 2012. Optical approaches to examining the dynamics of dissolved organic carbon in optically complex inland waters. *Environ. Res. Lett.* 7 (3), 034014.
- Knap, A.H., Michaels, A.F., Close, A.R., Ducklow, H.W., Dickson, A.G., 1996. Protocols for the joint global ocean flux study (JGOFS) core measurements. *JGOFS* 119–142.
- Kutser, T., 2012. The possibility of using the Landsat image archive for monitoring long time trends in coloured dissolved organic matter concentration in lake waters. *Remote Sens. Environ.* 123, 334–338.
- Li, J., Zhang, Y., Ma, R., Duan, H., Loisselle, S., Xue, K., Liang, Q., 2017. Satellite-based estimation of column-integrated algal biomass in nonalgal bloom conditions: a case study of Lake Chaohu, China. *IEEE J. Sel. Top. Appl. Earth Obs. Remote Sens.* 10, 450–462.
- Liu, D., Bai, Y., He, X., Pan, D., Wang, D., Wei, J.-A., Zhang, L., 2018. Dynamic observation of dissolved organic matter in the Pearl River Estuary, China, from space. *Acta Oceanol. Sin.* 37, 105–117.
- Liu, D., Pan, D., Bai, Y., He, X., Wang, D., Zhang, L., 2015. Variation of dissolved organic carbon transported by two Chinese rivers: the Changjiang River and Yellow River. *Mar. Pollut. Bull.* 100, 60–69.
- Ludwig, W., Probst, J.-L., 1996. Predicting the oceanic input of organic carbon by continental erosion. *Glob. Biogeochem. Cycles* 10, 23–41.
- Ma, R., Duan, H., Hu, C., Feng, X., Li, A., Ju, W., Jiang, J., Yang, G., 2010. A half-century of changes in China's lakes: global warming or human influence? *Geophys. Res. Lett.* 37.
- Manahan, D.T., Crisp, D.J., 1982. The role of dissolved organic material in the nutrition of Pelagic Larvae: amino acid uptake by bivalve veligers. *Am. Zool.* 22, 635–646.
- Mendonça, R., Muller, R.A., Clow, D., Verpoorter, C., Raymond, P., Tranvik, L.J., Sobek, S., 2017. Organic carbon burial in global lakes and reservoirs. *Nat. Commun.* 8, 1694.
- Mladenov, N., Pulido-Villena, E., Morales-Baquero, R., Ortega-Retuerta, E., Sommaruga, R., Reche, I., 2008. Spatiotemporal drivers of dissolved organic matter in high alpine lakes: role of Saharan dust inputs and bacterial activity. *J. Geophys. Res.: Biogeosciences* 113.
- Morel, A., Gentili, B., 2009. A simple band ratio technique to quantify the colored dissolved and detrital organic material from ocean color remotely sensed data. *Remote Sens. Environ.* 113, 998–1011.
- Mueller, J.L., Fargion, G.S., McClain, C.R., 2003. *Ocean Optics Protocols for Satellite Ocean Color Sensor Validation, Revision 4, Volume III: Radiometric Measurements and Data Analysis Protocols*, NASA/TM-2003-211621/Rev4-Vol. III. NASA Goddard Space Flight Center, Greenbelt, Maryland, p. 78.
- Oubelkheir, K.J., Claustre, H., Sciandra, A., Babin, M., 2005. Bio-optical and biogeochemical properties of different trophic regimes in oceanic waters. *Limnol. Oceanogr.* 50, 1795–1809.
- Qin, B., 2002. Approaches to mechanisms and control of eutrophication of shallow lakes in the middle and lower reaches of the Yangtze River. *J. Lake Sci.* 14, 193–202.
- Safieddine, S.A., Heald, C.L., 2017. A global assessment of dissolved organic carbon in precipitation. *Geophys. Res. Lett.* 44 (11), 672–611,681.
- Seitzinger, S.P., Harrison, J.A., Dumont, E., Beusen, A.H.W., Bouwman, A.F., 2005. Sources and delivery of carbon, nitrogen, and phosphorus to the coastal zone: an overview of Global Nutrient Export from Watersheds (NEWS) models and their application. *Glob. Biogeochem. Cycles* 19.
- Shangguan, W., Dai, Y., Liu, B., Ye, A., Yuan, H., 2012. A soil particle-size distribution dataset for regional land and climate modelling in China. *Geoderma* 171–172, 85–91.
- Shi, K., Zhang, Y., Xu, H., Zhu, G., Qin, B., Huang, C., Liu, X., Zhou, Y., Lv, H., 2015. Long-term satellite observations of microcystin concentrations in Lake Taihu during cyanobacterial bloom periods. *Environ. Sci. Technol.* 49, 6448–6456.
- Siegel, D.A., Maritorena, S., Nelson, N.B., Hansell, D.A., Lorenzi-Kayser, M., 2002. Global distribution and dynamics of colored dissolved and detrital organic materials. *J. Geophys. Res.: Oceans* 107 (C12), 3228.
- Sobek, S., Tranvik, L.J., Prairie, Y.T., Kortelainen, P., Cole, J.J., 2007. Patterns and regulation of dissolved organic carbon: an analysis of 7500 widely distributed lakes. *Limnol. Oceanogr.* 52, 1208–1219.
- Stedmon, C.A., Markager, S., Søndergaard, M., Vang, T., Laubel, A., Borch, N.H., Windelin, A., 2006. Dissolved organic matter export to a temperature estuary: seasonal variations and implications of land use. *Estuar. Coasts* 29, 388–400.
- Sun, D.Y., Li, Y.M., Wang, Q., Lu, H., Le, C.F., Huang, C.C., Gong, S.Q., 2011. A neural-network model to retrieve CDOM absorption from in situ measured hyper-spectral data in an optically complex lake: lake Taihu case study. *Int. J. Remote Sens.* 32, 4005–4022.
- Swan, C.M., Nelson, N.B., Siegel, D.A., Fields, E.A., 2013. A model for remote estimation of ultraviolet absorption by chromophoric dissolved organic matter based on the global distribution of spectral slope. *Remote Sens. Environ.* 136, 277–285.
- Tiwari, S.P., Shanmugam, P., 2011. An optical model for the remote sensing of coloured dissolved organic matter in coastal/ocean waters. *Estuar. Coast Shelf Sci.* 93, 396–402.
- Tong, Y., Zhang, W., Wang, X., Couture, R.-M., Larssen, T., Zhao, Y., Li, J., Liang, H., Liu, X., Bu, X., He, W., Zhang, Q., Lin, Y., 2017. Decline in Chinese lake phosphorus concentration accompanied by shift in sources since 2006. *Nat. Geosci.* 10, 507–511.
- Wang, M., Liu, X., Zhang, J., 2002. Evaluate method and classification standard on lake eutrophication (in Chinese). *Environ. Monit. China* 18, 47–49.
- Wang, S., Li, J., Zhang, B., Spyros, E., Tyler, A.N., Shen, Q., Zhang, F., Kuster, T., Lehmann, M.K., Wu, Y., Peng, D., 2018. Trophic state assessment of global inland waters using a MODIS-derived Forel-Ule index. *Remote Sens. Environ.* 217, 444–460.
- Wang, X., Ma, H., Li, R., Song, Z., Wu, J., 2012. Seasonal fluxes and source variation of organic carbon transported by two major Chinese Rivers: the Yellow River and Changjiang (Yangtze) River. *Glob. Biogeochem. Cycles* 26.
- Weishaar, J.L., Aiken, G.R., Bergamaschi, B.A., Fram, M.S., Fujii, R., Mopper, K., 2003. Evaluation of specific ultraviolet absorbance as an indicator of the chemical composition and reactivity of dissolved organic carbon. *Environ. Sci. Technol.* 37, 4702–4708.
- Xia, B., Zhang, L., 2011. Carbon distribution and fluxes of 16 rivers discharging into the Bohai Sea in summer. *Acta Oceanol. Sin.* 30, 43–54.
- Xue, K., Ma, R., Duan, H., Shen, M., Boss, E., Cao, Z., 2019. Inversion of inherent optical properties in optically complex waters using sentinel-3A/OLCI images: a case study using China's three largest freshwater lakes. *Remote Sens. Environ.* 225, 328–346.
- Yao, B., Hu, C., Liu, Q., 2016. Fluorescent components and spatial patterns of chromophoric dissolved organic matters in Lake Taihu, a large shallow eutrophic lake in China. *Environ. Sci. Pollut. Control Ser.* 23, 23057–23070.
- Yue, T.X., Wang, Y.A., Liu, J.Y., Chen, S.P., Qiu, D.S., Deng, X.Z., Liu, M.L., Tian, Y.Z., Su, B.P., 2005. Surface modelling of human population distribution in China. *Ecol. Model.* 181, 461–478.
- Zhang, S., Liu, J., Wei, S., Gao, J., Wang, D., Zhang, K., 2006. Impact of aquaculture on

- eutrophication in changshou reservoir. *Chin. J. Geochem.* 25, 90–96.
- Zhang, Y., van Dijk, M.A., Liu, M., Zhu, G., Qin, B., 2009. The contribution of phytoplankton degradation to chromophoric dissolved organic matter (CDOM) in eutrophic shallow lakes: field and experimental evidence. *Water Res.* 43, 4685–4697.
- Zhang, Y., Zhang, B., Wang, X., Li, J., Feng, S., Zhao, Q., Liu, M., Qin, B., 2007. A study of absorption characteristics of chromophoric dissolved organic matter and particles in Lake Taihu, China. *Hydrobiologia* 592, 105–120.
- Zhang, Y., Zhang, E., Yin, Y., van Dijk, M.A., Feng, L., Shi, Z., Liu, M., Qina, B., 2010. Characteristics and sources of chromophoric dissolved organic matter in lakes of the Yungui Plateau, China, differing in trophic state and altitude. *Limnol. Oceanogr.* 55, 2645–2659.